CHEMISTRY OF MATERIALS
Article

Chem. Mater. **2010,** *22,* 6575–6582 6575
DOI:10.1021/cm1023579

Probing the Size Effect of Co_2FeGa-SiO_2@C Nanocomposite Particles Prepared by a Chemical Approach

Changhai Wang,[†] Lubna Basit,[†] Yuriy Khalavka,[‡] Yanzhi Guo,[†] Frederick Casper,[†] Teuta Gasi,[†] Vadim Ksenofontov,[†] Benjamin Balke,[†] Gerhard H. Fecher,[†] Carsten Sönnichsen,[‡] Yeu-Kuang Hwu,[§,∥] Jey-Jau Lee,[∥] and Claudia Felser*[,†]

[†]*Institute of Inorganic and Analytical Chemistry, Johannes Gutenberg University Mainz, 55099 Mainz, Germany,* [‡]*Institute of Physical Chemistry, Johannes Gutenberg University Mainz, 55128 Mainz, Germany,* [§]*Institute of Physics, Academia Sinica, 11529 Taipei, Taiwan, and* [∥]*National Synchrotron Radiation Research Center, 30076 Hsinchu, Taiwan*

Received August 17, 2010. Revised Manuscript Received November 12, 2010

In this contribution, we report the chemical synthesis of carbon coated, silica supported Co_2FeGa (Co_2FeGa-SiO_2@C) nanocomposite particles. The particle size of Co_2FeGa particles can be tuned by varying the amount of silica supports. The dependences of the crystal structure and magnetic properties on particle size have been investigated by synchrotron radiation based X-ray diffraction (XRD), X-ray absorption fine structure (XAFS) spectroscopy, transmission electron microscope (TEM), ^{57}Fe Mössbauer spectroscopy, and superconducting quantum interference device (SQUID). The superparamagnetic critical size of Co_2FeGa Heusler nanoparticles is found to be ~17 nm by correlating the TEM derived particle size distribution to the Mössbauer spectroscopy data. The effects of silica supports and carbon coating on the formation of Co_2FeGa nanoparticles of various sizes are also discussed.

Introduction

The concept of "nano" is inherently embedded in spintronics because the GMR (giant magneto resistance) effect which has given birth to spintronics was first discovered in multilayer structures with thickness reduced to nanoscale. Recently, efforts have been made to understand the effect of size on charge and spin transport properties of metallic nanoparticles.[1−3] Heusler compounds, first discovered in 1903, are special ferromagnets that can be made half-metallic with a high spin polarization up to 100%.[4] Heusler compounds are playing an increasingly important role in a wide span of application fields including spintronics,[5] solar cells,[6] thermoelectrics,[7] and topological insulators.[8] One of the most appealing merits of Heusler materials is that multifunctional properties can be materialized in one compound.[5] Recently Heusler compounds of reduced dimensionality have been emerged as model systems to study the interactions between size effect, nanomagnetism, and nanospintronics both theorectically[9] and experimentally.[10−12] Understanding the behavior of Heusler nanoparticles paves the way to technical innovations in spintronic devices to meet the increasing requirements of miniature, high performance, and energy-saving.

As for the synthesis of nanosized Heusler alloys, physical,[10,13] mechanical,[12] and chemical[14,15] methods have been reported. Ni−Mn−Ga films with an average grain size of ~70 nm have been prepared by pulsed laser deposition and exhibited an anomalous magneto resistance.[10] Heusler Fe_3Si nanoparticles (30 nm) have been fabricated by a modified sputtering method and the X-ray diffraction (XRD) analysis indicated the formation of the DO_3 ordered Fe_3Si phase.[13] Wang et al. prepared 10 nm Ni_2MnGa Heusler nanoparticles by ball milling and investigated the crystal structure and magnetic properties

*Corresponding author. E-mail: felser@uni-mainz.de.

(1) Black, C. T.; Murray, C. B.; Sandstrom, R. L.; Sun, S. H. *Science* **2000**, *290*, 1131.
(2) Yakushiji, K.; Ernult, F.; Imamura, H.; Yamane, K.; Mitani, S.; Takanashi, K.; Takahashi, S.; Maekawa, S.; Fujimori, H. *Nat. Mater.* **2004**, *4*, 57.
(3) Bernand-Mantel, A.; Seneor, P.; Lidgi, N.; Munoz, M.; Cros, V.; Fusil, S.; Bouzehouane, K.; Deranlot, C.; Vaures, A.; Petroff, F.; Fert, A. *Appl. Phys. Lett.* **2006**, *89*, 062502.
(4) Sakuraba, Y.; Hattori, M.; Oogane, M.; Ando, Y.; Kato, H.; Sakuma, A.; Miyazaki, T.; Kubota, H. *Appl. Phys. Lett.* **2006**, *88*, 192508.
(5) Felser, C.; Fecher, G. H.; Balke, B. *Angew. Chem. Int. Ed.* **2007**, *46*, 668.
(6) Kieven, D.; Klenk, R.; Naghavi, S.; Felser, C.; Gruhn, T. *Phys. Rev. B* **2010**, *81*, 075208.
(7) Barth, J.; Fecher, G. H.; Balke, B.; Graf, T.; Felser, C.; Shkabko, A.; Weidenkaff, A. *Phys. Rev. B* **2010**, *81*, 064404.
(8) Chadov, S.; Qi, X. L.; Kübler, J.; Fecher, G. H.; Felser, C.; Zhang, S. C. *Nat. Mater.* **2010**, *9*, 541.
(9) Zayak, A. T.; Beckman, S. P.; Tiago, M. L.; Entel, P.; Chelikowsky, J. R. *J. Appl. Phys.* **2008**, *104*, 074307.
(10) Golub, V. O.; Vovk, A. Ya.; Malkinski, L.; O'Connor, C. J.; Wang, Z.; Tang, J. *J. Appl. Phys.* **2004**, *96*, 3865.
(11) Ishikawa, T.; Marukame, T.; Matsuda, K.; Uemura, T.; Arita, M.; Yamamoto, M. *J. Appl. Phys.* **2006**, *99*, 08J110.
(12) Wang, Y. D.; Ren, Y.; Nie, H. Z.; Liu, D. M.; Zuo, L.; Choo, H.; Li, H.; Liaw, P. K.; Yan, J. Q.; Mcqueeney, R. J.; Richardson, J. W.; Huq, A. *J. Appl. Phys.* **2007**, *101*, 063530.
(13) Jing, Y.; Xu, Y. H.; Wang, J. P. *J. Appl. Phys.* **2009**, *105*, 07B520.
(14) Dahal, N.; Chikan, V. *Chem. Mater.* **2010**, *22*, 2892.
(15) Basit, L.; Wang, C. H.; Jenkins, C. A.; Balke, B.; Ksenofontov, V.; Fecher, G. H.; Felser, C.; Mugnaioli, E.; Kolb, U.; Nepijko, S. A.; Schöenhense, G.; Klimenkov, M. *J. Phys. D* **2009**, *42*, 084018.

© 2010 American Chemical Society
Published on Web 12/01/2010

of the nanoparticles.[12] Dahal et al. developed a colloidal approach for synthesizing 4 nm to ~7 nm Fe_3Si nanoparticles by reacting the preformed iron nanoparticles with silicon tetrachloride at 220 °C to ~250 °C.[14]

Among the numerous full Heusler compounds, Co based ones constitute the most promising candidates for spintronic applications due to their high spin polarization, high magnetization, and high Curie temperature.[16,17] Especially Co_2FeZ (Z = Al, Si) are presently used in the tunneling magneotoresistance (TMR) devices.[18−22] In comparison, the major interests in Ni_2MnGa nanoparticles go for ferromagnetic shape memory alloys (FSMA).[23−25] For Fe_3Si nanoparticles, the DO_3 ordered phase is not favorable for achieving a higher degree of spin polarization (a $L2_1$ or B_2 structure is optimal for this purpose).[26,27] For Co_2FeZ (Z = Al, Si, Ga, Ge) Heusler compounds, Si containing Heusler nanoparticles are not easy to chemically synthesize for their difficulty to reduce. Bulk Co_2FeAl, on the other hand, tends to adopt a disordered structure. Co−Mn based Heusler compounds are also suitable materials for spintronic devices due to their robust half metallicity.[28] However, the strong tendency of Mn to oxidize renders difficulty in obtaining pure Heusler phase.

Recently, we reported the chemical synthesis of Co_2FeGa Heusler nanoparticles in the presence of silica supports.[15] This synthesis is a modified impregnation-calcination method that has been investigated for binary alloy nanoparticles such as FeCo[29] and FePt.[30] We extended this approach to ternary Co_2FeGa nanoparticles considering the similarities in electronegativity and atomic radius of Fe, Co, and Ga. It is also noted that, using the same synthetic approach as with Co_2FeGa nanoparticles, the chemical syntheses of Co_2FeAl, Co_2FeSi, and Co_2MnGa nanoparticles have been attempted with less success. Therefore, Co_2FeGa seems to be a good candidate for the chemical synthesis of ternary Heusler nanoparticles for spintronic applications.

Particle size plays a critical role in determining the structure, biological, physical, and chemical properties of technologically oriented nanoparticles.[31−34] In this work, Co_2FeGa-SiO_2@C nanocomposite particles with a variety of sizes of Co_2FeGa phase are prepared and the size dependences of the crystal structure and magnetic properties are investigated. Furthermore, the superparamagnetic size limit of the Co_2FeGa Heusler nanoparticles is determined by correlating the transmission electron microscopy (TEM) derived particle size distribution to the Mössbauer spectroscopy data. A successful chemical preparation of Co_2FeGa nanoparticles with controlled particle size makes it possible to understand the size dependent physical properties of Heusler compounds at the nanoscale.

Experimental Section

Chemicals and Synthesis. Co_2FeGa-SiO_2@C nanocomposite particles were synthesized based on the reported method[15] with some modifications. All the chemicals were purchased from Sigma-Aldrich and used as received. The precursors were $Fe(NO_3)_3 \cdot 9H_2O$ (99.99%), $CoCl_2 \cdot 6H_2O$ (> 99%), and $Ga(NO_3)_3 \cdot xH_2O$ (99.9%). The value of x in $Ga(NO_3)_3 \cdot xH_2O$ was adopted as 8 for the calculation according to the literature.[35] The silica supports were commercially available fume silica (average size of 20 nm). In a typical preparation, 0.40 mmol of $Fe(NO_3)_3 \cdot 9H_2O$, 1.08 mmol of $CoCl_2 \cdot 6H_2O$, and 0.32 mmol of $Ga(NO_3)_3 \cdot xH_2O$ were dispersed in 50 mL of methanol and treated by a mild sonication for 5 min. Silica spheres of a variety of weights (0.5 g, 1.0 g, 1.5 g) were added to the precursor solution, and the suspension was sonicated for 1 h. Methanol was removed using a rotary evaporator. The obtained solid was dried at 80 °C for 2 h to achieve complete dryness. The solid was gently grounded to a powder, and typically 200 mg was used for annealing (850 °C for 5 h) under H_2 atmosphere with a flow rate of 50 mL/min. To stabilize the formed Co_2FeGa nanoparticles, the H_2 flow was switched to a methane flow (100 mL/min) at the end of annealing and maintained for 5 min. The samples were naturally cooled to room temperature and collected for analysis. Polycrystalline bulk Co_2FeGa samples were prepared by arc melting of stoichiometric amounts of high purity elements in an argon atmosphere at a pressure of 10^{-4} mbar. The bulk Co_2FeGa compound was annealed in an evacuated quartz tube for 1 week.[36]

Structural Characterization. The crystal structure of Co_2FeGa-SiO_2@C nanocomposite particles was investigated by synchrotron radiation based powder X-ray diffraction (XRD) at the beamline SP12B2 of Spring 8 (Hyogo, Japan). The photon energy was 7.12 keV. The stoichiometry of the samples were obtained by comparing the edge jumps in the X-ray absorption

(16) Balke, B.; Wurmehl, S.; Fecher, G. H.; Felser, C.; Kübler, J. *Sci. Technol. Adv. Mater*. **2008**, *9*, 014102.
(17) Trudel, S.; Gaier, O.; Hamrle, J.; Hillebrands, B. *J. Phys. D: Appl. Phys*. **2010**, *43*, 193001.
(18) Gercsi, Z.; Rajanikanth, A.; Takahashi, Y. K.; Hono, K.; Kikuchi, M.; Tezuka, N.; Inomata, K. *Appl. Phys. Lett*. **2006**, *89*, 082512.
(19) Ebke, D.; Schmalhorst, J.; Liu, N.-N.; Thomas, A.; Reiss, G.; Hütten, A. *Appl. Phys. Lett*. **2006**, *89*, 162506.
(20) Tezuka, N.; Ikeda, N.; Sugimoto, S.; Inomata, K. *Appl. Phys. Lett*. **2006**, *89*, 252508.
(21) Tezuka, N.; Okamura, S.; Miyazaki, A.; Kikuchi, M.; Inomata, K. *J. Appl. Phys*. **2006**, *99*, 03T314.
(22) Marukame, T.; Ishikawa, T.; Hakamata, S.; Matsuda, K.-I.; Uemura, T.; Yamamoto, M. *Appl. Phys. Lett*. **2007**, *90*, 012508.
(23) Ullakko, K.; Huang, J. K.; Kanter, C.; Kokorin, V. V.; O'Handley, R. C. *Appl. Phys. Lett*. **1996**, *69*, 1966.
(24) Sozinov, A.; Likhachev, A. A.; Lanska, N.; Ullakko, K. *Appl. Phys. Lett*. **2002**, *80*, 1746.
(25) Takeuchio, I.; Famodu, O.; Read, J. C.; Aronova, M. A.; Chang, K.-S.; Craciunescu, C.; Lofland, S. E.; Wuttig, M.; Wellstood, F. C.; Knauss, L.; Orozco, A. *Nat. Mater*. **2003**, *2*, 180.
(26) Block, T.; Felser, C.; Jakob, G.; Ensling, J.; Muhling, B.; Gutlich, P.; Beaumont, V.; Studer, F.; Cava, R. J. *J. Solid State Chem*. **2003**, *176*, 646.
(27) Elmers, H. J.; Fecher, G. H.; Valdaitsev, D.; Nepijko, S. A.; Gloskovskii, A.; Jakob, G.; Schöenhense, G.; Wurmehl, S.; Block, T.; Felser, C.; Hsu, P. C.; Tsai, W. L.; Cramm, S. *Phys. Rev. B* **2003**, *67*, 104412.
(28) Galanakis, I.; Özdoğan, K.; Aktas, B.; Sasıoğlu, E. *Appl. Phys. Lett*. **2006**, *89*, 042502.
(29) Seo, W. S.; Lee, J. H.; Sun, X. M.; Suzuki, Y.; Mann, D.; Liu, Z.; Terashima, M.; Yang, P. C.; McConnell, M. V.; Nishimura, D. G.; Dai, H. J. *Nat. Mater*. **2006**, *5*, 971.
(30) Seo, W. S.; Kim, S. M.; Kim, Y. M.; Sun, X. M.; Dai, H. J. *Small* **2008**, *4*, 1968.
(31) Matthias, F.; Marc, A. *Chem. Mater*. **2009**, *21*, 5886.
(32) Jiang, W.; Kim, B. Y. S.; Rutka, J. T.; Chan, W. C. W. *Nat. Nanotechnol*. **2008**, *3*, 145.
(33) Campbell, C. T.; Parker, S. C.; Starr, D. E. *Science* **2002**, *298*, 811.
(34) Rong, C. B.; Li, D.; Nandwana, V.; Poudyal, Y.; Ding, Y.; Lin, Z.; Wang, Z. L.; Zeng, H.; Liu, J. P. *Adv. Mater*. **2006**, *18*, 2984.
(35) Jung, W. S. *Bull. Korean Chem. Soc*. **2004**, *25*, 51.
(36) Balke, B.; Wurmehl, S.; Fecher, G. H.; Felser, C.; Alves, M. C. M.; Bernardi, F.; Morais, J. *Appl. Phys. Lett*. **2007**, *90*, 172501.

spectra following the general procedures reported in the literature.[37] X-ray absorption fine structure (XAFS) measurements were performed at BL17C1 of the National Synchrotron Radiation Research Center (NSRRC, Hsinchu, Taiwan). The spectra of the samples were collected in the transmission mode. A transmission electron microscope (TEM) Philips EM420 was used for the investigation of particle morphology, size, and distributions. High-resolution TEM (HRTEM), scanning TEM (STEM), and energy dispersive X-rays (EDX) measurements were performed using a FEI Tecnai F 30 TEM, equipped with a field emission gun. For TEM sample preparation, individually dispersed Co_2FeGa nanoparticles were obtained by dissolving silica using 10% aq hydrofluoric acid (HF) solution for 1 h. The suspended nanoparticles were collected by centrifugation (16 000 rpm, 20 min), washed, and redispersed in ethanol. Several drops of the solutions were loaded on a carbon coated copper grid for TEM measurements. The average particle size was evaluated by counting more than 200 individual particles.

Magnetic Characterization. The magnetic properties of Co_2FeGa-SiO_2@C nanocomposite particles were measured by a superconducting quantum interference device (SQUID, Quantum Design MPMS-XL-5). ^{57}Fe Mössbauer measurements were performed using a conventional, constant-acceleration spectrometer at room temperature. For excitation, a ^{57}Co source was used to deliver γ radiation with a photon energy of 14.4 keV. The Mössbauer data were analyzed using the program RECOIL.[38] Isomer shifts were presented with respect to bcc Fe foil. It is noted that, except for TEM, Co_2FeGa-SiO_2@C nanocomposite particles, instead of free-standing Co_2FeGa nanoparticles, were utilized for structural and magnetic characterizations. To extract the magnetic response of Co_2FeGa nanoparticles, the weight fractions of Co_2FeGa in the nanocomposite samples were measured by atomic absorption spectroscopy (AAS) and were used for magnetization calculations.

Results and Discussion

Structure of $L2_1$ Ordered Carbon Coated Co_2FeGa Nanoparticles. The composition, structure, and magnetic properties of Co_2FeGa-SiO_2@C nanocomposite particles are summarized in Table 1. As shown in Figure 1a−d, the particle size depends on the amount of silica supports in sample preparation, i.e., the more silica added, the smaller particle size obtained. For sample A, a broad particle distribution appears with sizes ranging from 40 to 120 nm. Increasing the silica weight to 1 g, the Co_2FeGa nanoparticles are smaller with improved size dispersion (17.9 ± 5.3 nm). For sample C, however, a bimodal distribution of nanoparticles is observed and both larger (36.7 nm in average) and smaller (7 nm in average) particles coexist. Without HF etching (see Figure 1e), the phase contrast between Co_2FeGa and SiO_2 is poor. Therefore HF etching is necessary to evaluate the particle size distribution of Co_2FeGa nanoparticles using TEM. The dependence of the particle size on the amount of silica supports is shown in Figure 1f.

As shown in Figure 2a, a HRTEM probe on sample B reveals a single crystalline domain with a planar spacing of 0.203 nm corresponding to the (220) planes. This confirms the high crystallinity of the particles. Carbon shells encapsulating the Co_2FeGa nanoparticles were observed that consist of 2−3 layers. The carbon layers are observed more clearly from a snapshot in Figure 2b. The spacing of the carbon lattice fringes is 0.33 nm, which is close to the reported interplanar distance of graphite (0001) planes.[39,40] Selected EDX data indicate a slight fluctuation of Co/Fe ratios centering at 2:1 and deficient Ga in all samples. The EDX derived compositions are comparable with that determined by analyzing the XAFS spectra. The compositions of individual particles were

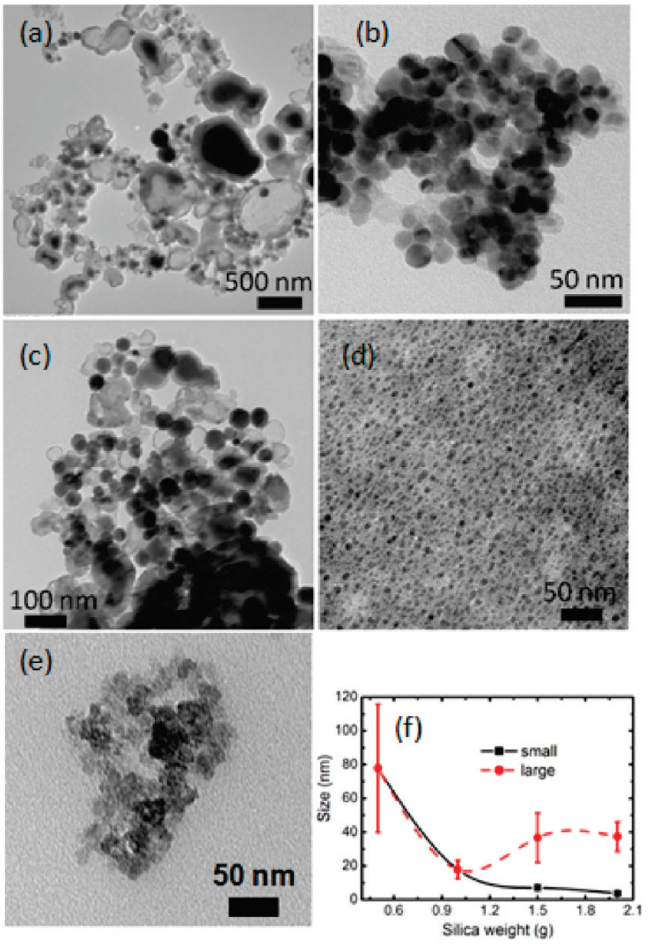

Figure 1. TEM micrographs of the carbon coated Co_2FeGa nanoparticles with various sizes obtained by HF etching: (a) sample A; (b) sample B; (c, d) sample C. Micrograph of the nonetched sample B is shown in part e. The particle size and distribution as a function of silica weight is shown in part f. Dashed and solid lines are guides to the eye.

Table 1. Composition, Structural, and Magnetic Properties of Co_2FeGa Samples at RT

ID	composition	a^a [Å]	$d_m{}^b$ [nm]	$M_s{}^c$ [emu/g]	$H_c{}^c$ [Oe]	$B_r{}^c$ [emu/g]	H_{hff} [kOe]	IS [mm s^{-1}]	doublet [V %]	sextet [V %]	K [J/m^3]
A	$Co_{2.0}Fe_{1.12}Ga_{0.72}$	5.723	77.8 ± 37.9	111.7	40.0	2.25	319.0	0.052	17.8	82.2	193
B	$Co_{2.0}Fe_{1.09}Ga_{0.66}$	5.722	17.9 ± 5.3	114.2	38.8	1.28	319.4	0.062	18.7	81.3	15 900
C	$Co_{2.0}Fe_{1.01}Ga_{0.60}$	5.717	bimodal^d	110.6	302	14.6	318.9	0.055	27.7	72.3	4 800

^{a} Lattice constant. ^{b} TEM derived particle size. ^{c} At T = 5 K. ^{d} Bimodal size.

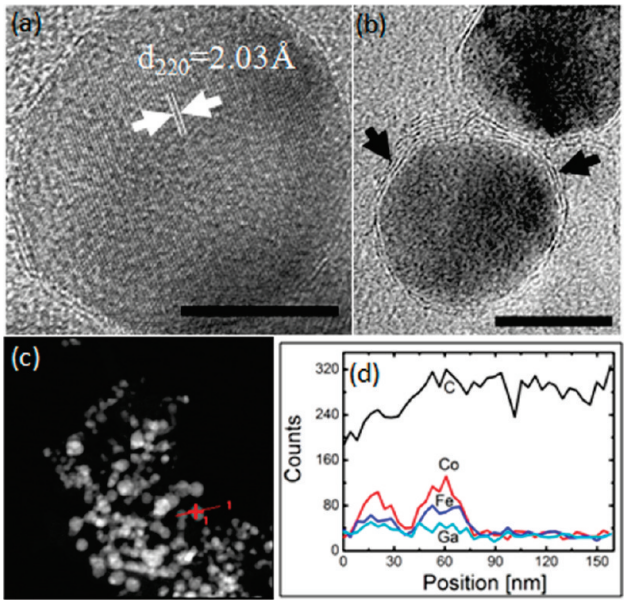

Figure 2. HRTEM (a,b), STEM micrographs (c), and EDX line profile (d) of the carbon coated Co_2FeGa nanoparticles (sample C). The arrows in part b indicate the graphite layers at the particle surface. Scale bars, 10 nm.

also examined by line scans for two adjacent nanoparticles. As shown in Figure 2c,d, it is noted that the iron content of the probed particles varies drastically. The deviation of iron composition from the nominal value might be attributed to the uneven distribution of metals within the particle at the nanoscale and/or the presence of metal impurities as discussed below.

Figure 3a shows the XRD patterns of Co_2FeGa-SiO_2@C nanocomposite particles of various particle sizes. With the comparison of the appearance and relative intensities of (111) and (200) reflections, various types of disordered phase of Heusler compounds can be identified.[41] Among the fcc fingerprint (111) and (200) reflections associated with the $L2_1$ crystal structure, only the (111) peaks were observable for samples A and B (see the inserts in Figure 3b). Thus, the formation of the A2 or B2 phase is excluded. Neither (111) nor (200) reflection was observed for sample C that might be due to the size-induced broadening. To unambiguously identify the $L2_1$ ordered structure, anomalous XRD (AXRD) and extended X-ray absorption fine structure (EXAFS) are valuable tools as reported in previous work.[15,42] AXRD measurements were performed on sample A to verify the $L2_1$ Heusler structure. Both (111) and (200) reflections were examined. This approach is different from the reported approach for Co_2MnGe Heusler films where only the (111) reflection was examined.[42] For the $L2_1$

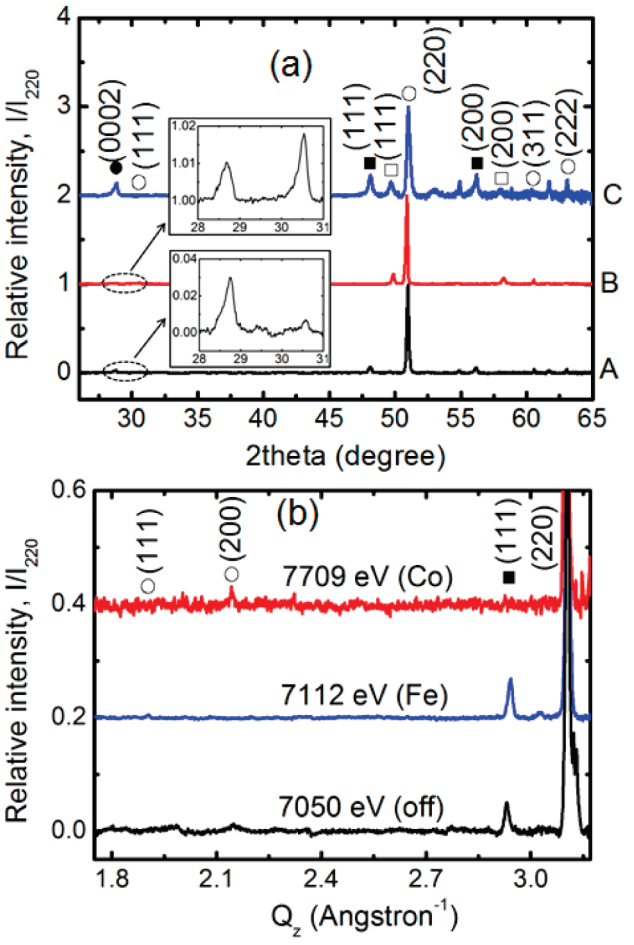

Figure 3. XRD patterns of the carbon coated Co_2FeGa nanoparticle samples A−C: (a) synchrotron radiation XRD patterns using a photon energy of 7.12 keV. Inserts in part a show the zoom-in of 2θ range of 28−31°; (b) anomalous XRD patterns of sample A at photon energies of 7112, 7709, and 7705 eV. Q_z is the momentum transfer and defined by $Q_z = 2\pi/d$. d is the interplanar spacing. Symbols in (a) ●, graphite; ○, Co_2FeGa; ■, Fe; □, Co.

ordered Co_2FeGa with a *Fm*-3*m* symmetry, structural scattering amplitudes of the first three permitted Bragg reflections are given by $F_{(111)} = 4|f_{Ga} - f_{Fe}|$, $F_{(200)} = 4|f_{Ga} + f_{Fe} - 2f_{Co}|$, and $F_{(220)} = 4|f_{Ga} + f_{Fe} + 2f_{Co}|$, where f_{Co}, f_{Fe}, and f_{Ga} are atomic scattering factors of the constituent atoms. The amplitude of atomic scattering factors is affected by the photon energy and it becomes small when the photon energy is close to the absorption edge of the specific atoms. This enhances either (111) or (200) reflection when the X-ray energy approaches to the K edges of Fe or Co. As shown in Figure 3b, the (111) intensity is enhanced at 7112 eV and an increase in the intensity of the (200) reflections is observed at an energy of 7709 eV. Under the off-resonant condition with a photon energy of 7705 eV, neither reflection is enhanced. The lattice constants were calculated (see Table 1) and were smaller compared to the reported value for bulk Co_2FeGa.[43] The (0002) reflections of hexagonal graphite were observed in all samples confirming the carbon coating. No diffraction peak belonging to either metallic carbide or

(37) Lee, H.-Y.; Wu, T.-B.; Lee, J.-F. *J. Appl. Phys.* **1996**, *80*, 2176.
(38) Lagarec, K.; Rancourt, D. G. *Nucl. Instrum. Meth. Phys. Res., Sect. B* **1997**, *129*, 266.
(39) Gamlen, P. H.; White, J. W. *J. Chem. Soc. Faraday Trans. 2* **1976**, *72*, 446.
(40) Khalavka, Y.; Ohm, C.; Sun, L.; Banhart, F.; Sönnichsen, C. *J. Phys. Chem. C* **2007**, *111*, 12886.
(41) Graf, T.; Casper, F.; Winterlik, J.; Balke, B.; Fecher, G. H.; Felser, C. *Z. Anorg. Allg. Chem.* **2009**, *635*, 976.
(42) Ravel, B.; Cross, J. O.; Raphael, M. P.; Harris, V. G.; Ramesh, R.; Saraf, V. *Appl. Phys. Lett.* **2002**, *81*, 2812.
(43) Buschow, K. H. J.; Van Engen, P. G.; Jongebreur, R. *J. Magn. Magn. Mater.* **1983**, *38*, 1.

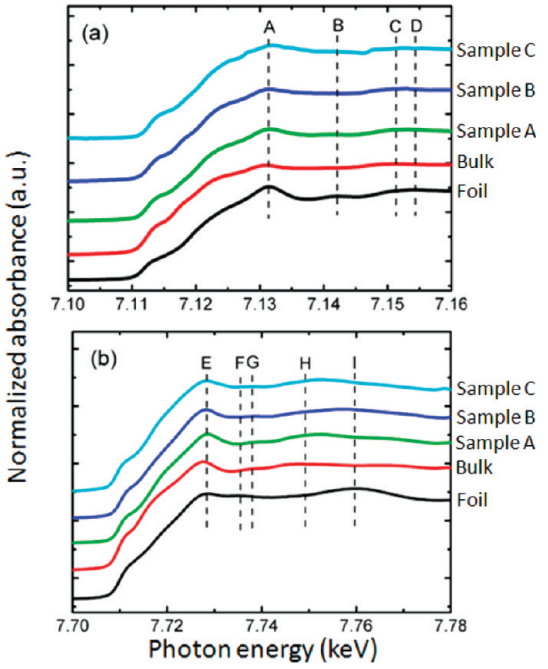

Figure 4. XANES spectra of metal foils, bulk Co_2FeGa, and Co_2FeGa nanoparticles A−C at the absorption K edges of Fe (a) and Co (b). The vertical lines are guides to the eye.

silicate was observed. Furthermore, impurity phases composed of fcc iron and fcc Co are observed in all samples. The presence of the Co impurities in Fe−Co nanoparticles has been reported in the literature.[29]

The X-ray absorption near edge structure (XANES) spectra of metal foils, bulk Co_2FeGa, and Co_2FeGa-SiO_2@C particles at the K edges of iron and cobalt are shown in Figure 4. The edge positions are determined from the first maximum of the first derivative spectra. Compared to edge positions of the metal foils, the absorption edges of bulk and nanoparticles show some positive energy shifts in a range of 0.5−0.9 eV. For the K edges of transition metals, a typical amplitude of energy shift for each increase in the oxidation by one valence unit is 2−3 eV.[44] This indicates that all the iron and cobalt species exist in zero-valence state within experimental error and the formation of iron or cobalt oxides is excluded.

As described in Figure 4a, the iron local atomic environment in bulk Co_2FeGa is featured with the "white line" at 7131.1 eV (A), followed by a platform ranging from 7135.6 to 7142.3 eV and a broadened hump centering at 7151.4 eV (C). The XANES spectra of the nanoparticles exhibit similar peak patterns within the first 40 eV above the edge, which supports the formation of the intermetallic compound. Furthermore, the characteristic resonances of bcc iron at 7142.1 eV (B) and 7154.4 eV (D) were not observed in the samples. This further supports the above argument. A similar scenario is observed at the Co K edge as displayed in Figure 4b. The spectroscopic feature of Co in bulk Co_2FeGa can be described by the "white line" 7728.0 eV (E) and two resonance peaks at 7737.9 eV (G) and 7749.2 eV (H). Samples A−C display similar characteristics compared to that of the bulk Co_2FeGa even though the G and H resonances damp in intensity and shift to higher photon energy. Again, the absence of characteristic resonances associating with hcp cobalt at 7735.4 eV (F) and 7749.2 eV (I) confirms the formation of the intermetallic Co_2FeGa.

The formation of Co_2FeGa-SiO_2@C nanocomposite particles might involve several steps including loading the metal precursors within a porelike structure, high temperature reduction/alloying, and subsequent carbon coating. After solvent removal, the metal loaded silica opals are condensed and the silica particles formed pore structures. Under high temperature annealing under H_2 atmosphere, the metal precursors accommodated in such interparticle voids are transformed to nanoparticles. The graphite layers are deposited onto the particle surfaces by a chemical vapor deposition (CVD) process using methane. A vapor−liquid−solid mechanism of carbon coating has been proposed by Elliott and co-workers.[45] The role of the silica nanospheres in tuning the particle size of the formed nanoparticles has been less investigated. It is assumed that increasing the amount of silica nanospheres might decrease the concentration of the precursors. As reported by Seo et al.,[29] the average particle size decreased from 7 to 4 nm with a 4-fold decrease in the precursor concentration for Fe−Co nanoparticles. However, larger Co_2FeGa nanoparticles were obtained in this study and a bimodal dispersion pattern developed at a higher silica load. This might be attributed to the higher concentration of the precursors in our approach. A higher precursor concentration might be associated with the unevenly distributed precursors and the formation of nanoparticles with a broad size distribution. Further efforts are underway to clarify the role of the silica supports in controlling particle size and to improve size distribution.

Size Dependent Magnetic Properties. The size dependent magneto-structural correlations in Co_2FeGa nanoparticles were investigated by Mössbauer spectroscopy and a SQUID magnetometer. The Mössbauer spectra of samples A−C were measured at room temperatures and the results are shown in Figure 5 and summarized in Table 1. For samples A and C, a distribution fit model is absolutely necessary which corresponds properly to the features of these samples. Sample B exhibits a relatively narrow size distribution, and even a conventional Lorentzian profile model could be applied. All spectra were fitted by a superposition of one magnetic sextet (in distribution model) and one superparamagnetic doublet. The observed isomer shifts and hyperfine magnetic fields are close to the reported values for bulk Co_2FeGa[46] confirming the formation of the Heusler Co_2FeGa phase. The doublet/sextet intensity ratio steadily increases from samples A to C spanning the single and bimodal size domains.

(44) Waychunas, G. A.; Apted, M. J.; Brown, G. E., Jr. *Phys. Chem. Miner*. **1983**, *10*, 1.
(45) Elliott, B. R.; Host, J. J.; Dravid, V. P.; Teng, M. H.; Hwang, J. H. *J. Mater. Res*. **1997**, *12*, 3328.
(46) Jaggi, N. K.; Rao, K. R. P. M.; Grover, A. K.; Gupta, L. C.; Vijayaraghavan, R.; Dang, L. K. *Hyperfine Interact*. **1978**, *4*, 402.

A straightforward way to estimate the superparamagnetic size limit is not available for magnetic nanoparticles with a relatively broad size distribution. We propose an alternative way to pinpoint the critical size by relating the TEM-derived size and the Mössbauer spectroscopy data. This is exemplarily shown for sample B in Figure 6. First the particle size distribution pattern (see Figure 6a) is converted to a volume fraction pattern as a function of particle size. The size−volume fraction histogram is fitted with a Gaussian model as shown in Figure 6b. The integrated area below the Gaussian curve corresponds to the total amount of the nanoparticles. Taking into account of the fractions corresponding to the doublet (18.7%) and sextet (81.3%) subspectra, areas D and S can be identified in Figure 6c. The areas correspond to the amounts of particles under superparamagnetic and statically magnetic states, respectively. The particle size determined by the boundary (identified by a white arrow in Figure 6c) between the two areas is the superparamagnetic critical size and is found to be ~17 nm. This value is reasonable compared to a reported critical size of ~20 nm for $Fe_{40}Co_{60}$ nanoparticles.[29]

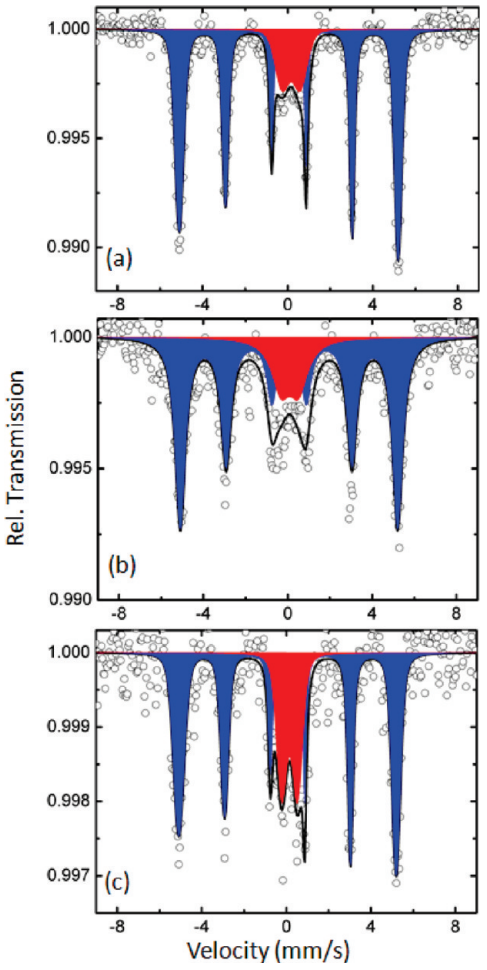

Figure 5. Mössbauer spectra of Co_2FeGa nanoparticles with various sizes at room temperature: (a) sample A; (b) sample B; (c) sample C. Superparamagnetic doublets and static magnetic sextets are shadowed by red and blue, respectively.

The magnetic behavior of Co_2FeGa nanoparticles was investigated by field and temperature dependent magnetometry. As shown in Figure 7a and Table 1, samples A and B demonstrate similar magnetization characteristics and are magnetically soft. The measured saturation magnetic moment at 5 K of the samples are in the range of 110 emu/g to ~114 emu/g (4.87 μ_B to ~4.97 μ_B), which are lower than the reported value for bulk Co_2FeGa (117.7 emu/g or 5.13 μ_B) at 4.2 K.[43] According to the Slater−Pauling rule, for the stoichiometric Co_2FeGa Heusler compound, the spin magnetic moment per unit cell value is 5μ_B/f.u. Therefore, the measured saturation magnetizations of Co_2FeGa nanoparticles were close to the Slater−Pauling value. On the other hand, the samples are nonstoichiometric with a Ga deficiency as described in Table 1. The nonstoichiometry induced antisite disorders in Co_2YZ (e.g., Y = Mn; Z = Si, Ge) have been investigated both theoretically[28,47] and experimentally.[48] As discussed previously,[49] the proposed antisite model for Ga-deficient Co_2FeGa nanoparticles was not supported by the magnetization results. It is assumed that the discussed formula unit antisite model is only applicable to Heusler compounds of a single phase. The presence of impurity phases introduces uncertainty in the actual phase composition and undermines the accuracy of the proposed antisite disorder model. The closeness of the measured magnetizations with the Slater−Pauling value might provide a hint that the stoichiometric Co_2FeGa phase was stabilized under nonstoichiometric conditions. The correlation between the particle size and magnetic moment of nanoparticles has been well studied and the saturation

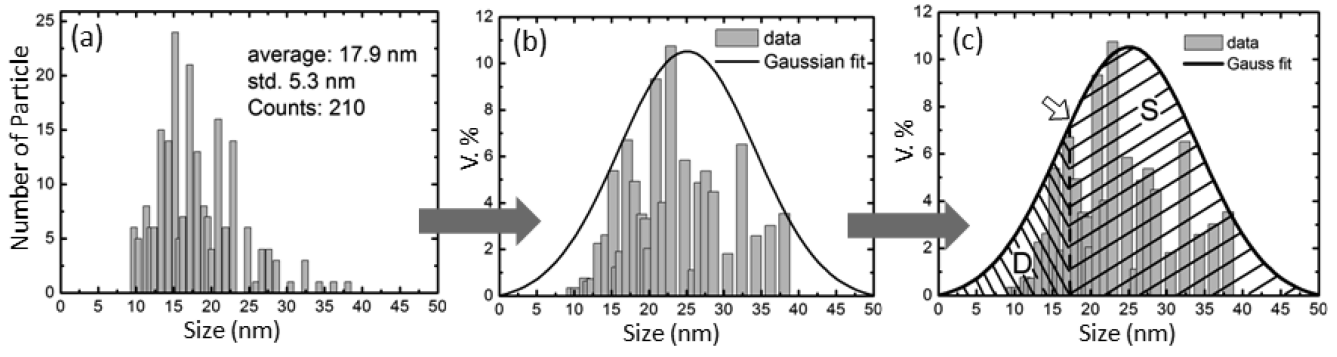

Figure 6. An illustration to determine the superparamagnetic critical size of Co_2FeGa nanoparticles: (a) particle size distribution; (b) volume percentage of the particles as a function of size; (c) determine the critical size by correlating to the volume fractions of doublet and sextet. The arrow in part c assigns the critical size of Co_2FeGa nanoparticles corresponding to the boundary between the doublet (D) and the sextet (S) areas.

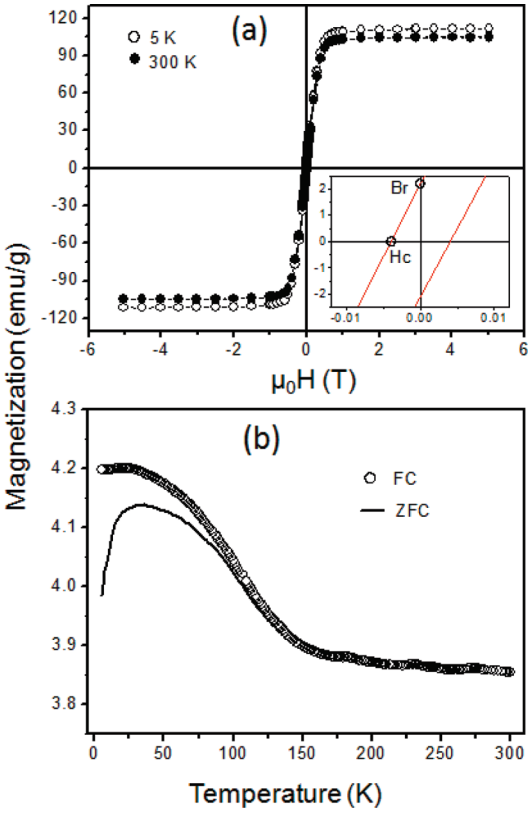

Figure 7. Magnetic properties of sample A: (a) magnetization curves at 5 and 300 K; (b) temperature dependent FC-ZFC curves. The insert in part a shows the hysteresis curves close to the origin on an enlarged scale.

magnetization normally decreases with decreasing particle size.[50,51] For Co_2FeGa nanoparticles, a biomodal particle distribution develops, the averaged particle size decreases, and the population of superparamagnetic nanoparticles increases. In this regard, our magnetization data are inconsistent with the decreasing rule of magnetization. At 5 K, the coercivities for samples A and B are close to 40 Oe. Sample C is also magnetically soft but with a larger coercivity.

Temperature dependent SQUID measurements were utilized to verify the superparamagnetic behavior of the smaller Co_2FeGa nanoparticles. Zero field cooled (ZFC) and field cooled (FC) magnetization curves have been measured for sample A in a temperature range of 5 K to ~300 K under a magnetic field of 0.01 T. As shown in Figure 7b, the blocking of sample A spread over a wide temperature range signifying a rather wide size distribution of particles. The magnetic susceptibility reaches a maximum at around 35.4 K corresponding to the contribution from the smallest particles in the sample. The temperature dependent Mössbauer spectroscopy of sample A was measured in a temperature range of 80 K to ~275 K.

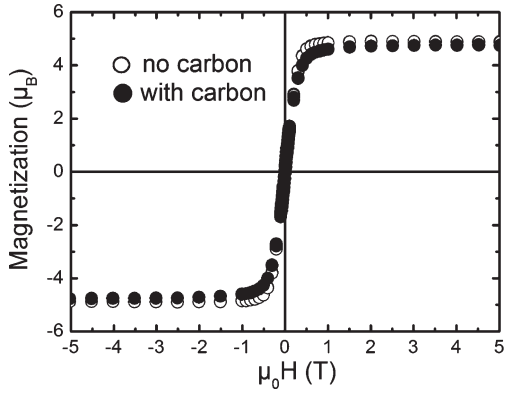

Figure 8. Magnetization curves of sample B under conditions with and without carbon coating. The methane CVD time is 5 min at a flow rate of 250 mL/min. Other sampling conditions are identical for the two samples.

In the examined temperature range, the fraction of the doublet decreased monotonously with decreasing temperature: 17.8% at 295 K, 13.4% at 275 K, 11.5% at 200 K, and 9.7% at 80 K, respectively. No sharp blocking temperature was observed, and a "blocking" process overspread a wide temperature range. This fact also corresponds to a broad distribution of particle size of this sample. The Mössbauer blocking temperature (BM) is defined as the temperature at which the fraction of the static component equals that of the superparamagnetic component. One can conclude that the BM of this sample should be well above room temperature. The blocking temperature determined from the magnetic measurement is lower than that determined from Mössbauer measurement. It could be explained by the different characteristic observation time of Mössbauer experiment ($\sim 10^{-8}$ s) and static magnetization measurements (~100 s).

The magnetic anisotropy of Co_2FeGa Heusler compound has not been extensively investigated. In this work, the effective anisotropy constant K for Co_2FeGa was calculated for the present samples. As predicted by the Néel−Arrhenius equation,[52] under superparamagnetic state, anisotropy constant K can be calculated by

$$K = \frac{k_B T \ln(\tau_m/\tau_0)}{V}$$

Herein, k_B is the Boltzmann constant, T is the Mössbauer blocking temperature, V is the particle volume. τ_m and τ_0 are the measured relaxation time and the relaxation constant taking the values of 10^{-8} and 10^{-13} s according to the literature.[53] The estimated BMs for samples A−C are taken as 300 K. The calculated effective anisotropy constants for samples A−C are listed in Table 1. The values for samples B and C are of same order in magnitude compared with the reported uniaxial anisotropy (K_u, 0.63×10^4 J/m^3) of Co_2FeSi Heusler thin films.[17,54]

(47) Picozzi, S.; Continenza, A.; Freeman, A. J. *Phys. Rev. B* **2004**, *69*, 094423.
(48) Yamamoto, M.; Ishikawa, T.; Taira, T.; Li, G. F.; Matsuda, K. I.; Uemura, T. *J. Phys.: Condens. Mater*. **2010**, *22*, 164212.
(49) Wang, C. H.; Guo, Y. Z.; Casper, F.; Balke, B.; Fecher, G. H.; Felser, C.; Hwu, Y. *Appl. Phys. Lett*. **2010**, *97*, 103106.
(50) Tang, Z. X.; Sorensen, C. M.; Klabunde, K. J.; Hadjipanayis, G. C. *Phys. Rev. Lett*. **1991**, *67*, 3602.
(51) Han, D. H.; Wang, J. P.; Luo, H. L. *J. Magn. Magn. Mater*. **1994**, *136*, 176.
(52) Goya, G. F.; Berquo, T. S.; Fonseca, F. C.; Morales, M. P. *J. Appl. Phys*. **2003**, *94*, 3520.
(53) Kodama, D.; Shinoda, K.; Sato, K.; Konno, Y.; Joseyphus, R. J.; Motomiya, K.; Takahashi, H.; Matsumoto, T.; Sato, Y.; Tohji, K.; Jeyadevan, B. *Adv. Mater*. **2006**, *18*, 3154.
(54) Hashimoto, M.; Herfort, J.; Schönherr, H.-P.; Ploog, K. H. *Appl. Phys. Lett*. **2005**, *87*, 102506.

Carbon coating is found effective to prevent Co_2FeGa nanoparticles from oxidation. The XRD data in Figure 3a indicate the absence of metal oxides in the final products. The surface immobilized carbon layers, however, are considered to decrease the spin polarization at the Fermi level and suppress the magnetization of the encapsulated magnetic nanoparticles.[55,56] In a control experiment, the saturation magnetization of samples were compared. As shown in Figure 8, the magnetic moment decreases from 4.89 to 4.77 μ_B in the presence of carbon layers. This observation is consistent with those reported in the literature.

Conclusions

In summary, we demonstrate a new approach to prepare Co_2FeGa-SiO_2@C nanocomposite particles. The size of Co_2FeGa nanoparticles can be tuned in a simple way by adjusting the amount of the silica supports. The formation of the $L2_1$ Co_2FeGa phase in the nanocomposite particles is confirmed by anomalous XRD, Mössbauer spectroscopy, and magnetic measurements. The variation of particle size affects the crystal structure and magnetic properties of Co_2FeGa nanoparticles. The correlation of TEM-derived particle size and Mössbauer spectroscopy specifies the critical size of Co_2FeGa nanoparticles bridging superparamagnetism and ferromagnetism. The role of silica spheres and carbon coating in controlling the size, structure, and magnetic properties of Co_2FeGa nanoparticles are also discussed. Further efforts are underway to improve the particle size distribution.

Acknowledgment. Financial support by the DFG is gratefully acknowledged (Project TP 2.3-A in research unit FOR 1464 "ASPIMATT"). The Synchrotron XRD and XAFS measurements were performed under the approvals of National Synchrotron Radiation Research Centre (NSRRC, Taiwan) under proposals of Grants 2009-1-102 and 2009-2-086, Grant BL12B2 at Spring 8 (Japan), and under proposals of Grants 2009A4131 and 2009B4128. Yuriy Khalavka is financially supported by MATCOR, a scholarship in the frame of the Graduate School of Excellence Mainz. Electron microscopy measurements are performed in the Electron Microscopy Centre Mainz (EMZM), partially financed by the SFB 625. We thank Dr. Ute Kolb, Dr. Tatiana Gorelik, and Rudolf Würfel for their assistance with the electron microscopic investigations.

(55) Weissmann, M.; Garcia, G.; Kiwi, M.; Ramirez, R. *Phys. Rev. B* **2004**, *70*, 201401.
(56) Ang, K. H.; Alexandrou, I.; Mathur, N. D.; Amaratunga, G. A. J.; Haq, S. *Nanotechnology* **2004**, *15*, 520.